Microstructure and Thermodynamics of Inhomogeneous Polymer Blends and Solutions

Sandeep Tripathi and Walter G. Chapman
Department of Chemical Engineering, Rice University, Houston, Texas, 77005, USA
(Received 3 April 2004; published 1 March 2005)

A free energy density functional theory (DFT) for nonuniform polymeric mixtures is proposed based on first order thermodynamic perturbation theory. The segment-density based free energy functional provides an accuracy comparable to the numerically intensive polymeric DFTs while preserving the computational simplicity of an atomic DFT. The presented applications for solutions and blends of branched and linear polymers demonstrate the capability of the theory to capture the entropic and enthalpic effects governing the microstructure.

DOI: 10.1103/PhysRevLett.94.087801 PACS numbers: 61.25.Hq, 61.20.Gy, 61.25.Em

The success of a density functional theory (DFT) for nonuniform polyatomic fluids rests with its choice of the ideal system and approximations for the excess free energy functional. Existing theories differ in the way the intramolecular interactions are split between the ideal and the excess contributions, and, accordingly, the compromise they offer between accuracy and computational expense. Absorbing the intramolecular energetics in the ideal system makes the theory less dependent on the excess term which can then be approximated either empirically [1], using bulk fluid structural information [2–4], or directly following from the functionals for atomic fluids [5,6]. However, this approach makes the theory computationally so demanding that a solution either requires computer simulations to solve for the exact ideal functional [2] or, when written in terms of multipoint molecular density $\rho(\mathbf{R})$ ($\mathbf{R} = \{\mathbf{r}_i\}$ where $\mathbf{r}_i$ is the position of bead i on the chain) [1,5–8], results in mth-order implicit integral equations for an m-mer system. The system of these equations requires a single chain simulation [7] or numerical techniques [6,8] that are computationally even more intensive than simulations [7]. Because of this mathematical challenge (and due to certain limitations), several problems of practical interest remain beyond their reach. The treatment of intramolecular interactions as an excess contribution simplifies the computations, but the approximation available for the excess contribution [9] fails to describe systems beyond those with a slowly varying external field. It is hence not applicable to strongly inhomogeneous systems such as polymer melts at surfaces [10].

In this Letter, we present a DFT that offers accuracy comparable to the molecular-density-based and simulation-dependent theories while retaining the form and computational simplicity of the atomic fluid DFTs (using the noninteracting ideal state). We demonstrate these features and the broad scope of the theory through applications of polymer adsorption in athermal and attractive systems, including the first DFT application to surface segregation in blends of chains of different architecture. Considering the polyatomic system as a mixture of associating spheres (in the limit of complete association), the free energy for the system is shown to follow naturally from the association free energy functionals based on first order thermodynamic perturbation theory (TPT1) [11] used with success in the DFTs for atomic associating fluids [12–14]. The appeal of the theory further reflects through its potential to address a wide range of applications (surfactants, bilayers, colloids, polyelectrolytes) within a common framework, and should thus interest chemical physicists, material and biological scientists, and engineers alike.

To describe a system of linear chains formed of m spherical segments, consider an m component mixture of associating spherical monomers that in the limit of infinitely strong association would form the desired system of chains. These monomers interact with a spherically symmetric intermolecular pair potential comprising a repulsive core and an attractive tail, and consist of surface association sites (two on each monomer that will make up the middle of the chain and one on each terminal segment). These association sites serve to bond successive segments on a chain through an additional short-ranged, directional square well interaction [12]. A similar approach is used in the statistical associating fluid theory (SAFT) of Chapman *et al.* [15] to describe the bulk state thermodynamics of molecular fluids. Any number of the m segments can be of the same type, but each unit is formally treated as a distinct specie, tagged along the chain backbone. To form branched chains, the segments at which the branch attaches to the chain backbone will have additional association sites to bond with the side groups. $\rho_\alpha^{\mathrm{seg}}(\mathbf{r})$ denotes the density of the αth segment at $\mathbf{r}$. The Helmholtz free energy of this associating mixture can be written as

$$A^{\mathrm{chain}} = A^{\mathrm{id}} + \Delta A^{\mathrm{EX}} + \Delta A^{\mathrm{assoc}}, \tag{1}$$

where the incremental terms represent free energy changes due to the excluded volume of the monomer segments and association between the segments in the mixture. A^{id} is the ideal gas free energy of the atomic mixture. ΔA^{EX} can be approximated in a weighted density formalism [16] using

any of the various accurate models available [17–19]. We have used Rosenfeld's functional [19] which is naturally derived for asymmetric mixtures. Following TPT1, ΔA^{assoc} can be written as [12]

$$\frac{\Delta A^{\text{assoc}}}{kT} = \int d\mathbf{r}_1 \sum_{\alpha=1}^{m} \rho_\alpha^{\text{seg}}(\mathbf{r}_1) \sum_{A}^{\{A\}} \left[\ln \chi_A^\alpha(\mathbf{r}_1) - \frac{\chi_A^\alpha(\mathbf{r}_1)}{2} + \frac{1}{2} \right]. \tag{2}$$

The summations, from left to right, are over the chain segments and the set of association sites on segment α, respectively. $\chi_A^\alpha(\mathbf{r})$ is the fraction of α segments at $\mathbf{r}$, not bonded at the association site A [12], which in the limit of complete association, would vanish throughout the system. In this limiting condition, we introduce the approximation $\chi_B^{\alpha'}(\mathbf{r}_2) \approx \chi_A^\alpha(\mathbf{r}_1)$, which essentially means that the extent of bonding at the sites on the adjacent segments α' and α approach the limit of complete bonding at the same rate. This leads to the following simplified expression for $\chi_A^\alpha(\mathbf{r})$ [12]

$$\chi_A^\alpha(\mathbf{r}_1)^2 = \frac{1 - \chi_A^\alpha(\mathbf{r}_1)}{\int d\mathbf{r}_2 \Delta^{\alpha\alpha'}(\mathbf{r}_1, \mathbf{r}_2) \rho_{\alpha'}^{\text{seg}}(\mathbf{r}_2)}, \tag{3}$$

where $\Delta^{\alpha\alpha'}(\mathbf{r}_1, \mathbf{r}_2) = y^{\alpha\alpha'}(\mathbf{r}_1, \mathbf{r}_2) F^{\alpha\alpha'}(\mathbf{r}_1, \mathbf{r}_2) K$. $y^{\alpha\alpha'}(\mathbf{r}_1, \mathbf{r}_2)$ is the cavity correlation function between the two segments α and α' in the reference fluid and K is a constant geometric factor accounting for the orientation of the two segments on bonding as given in [12–14]. For the association Mayer function [12–14], $F^{\alpha\alpha'}(\mathbf{r}_1, \mathbf{r}_2) = \{\exp[\beta \varepsilon_{as}^{\alpha\alpha'}(\mathbf{r}_1, \mathbf{r}_2)] - 1\}$, we can write $\varepsilon_{as}^{\alpha\alpha'}(\mathbf{r}_1, \mathbf{r}_2) = \varepsilon_0 - \nu_{\text{bond}}^{\alpha\alpha'}(\mathbf{r}_1, \mathbf{r}_2)$, where $\varepsilon_0 \to \infty$ in the limit of complete association and $\nu_{\text{bond}}^{\alpha\alpha'}(\mathbf{r}_1, \mathbf{r}_2)$ is the energy of the bond, e.g., harmonic bonding potential, between the two segments. Substituting in Eq. (2) and forcing the limit $\chi_A^\alpha(\mathbf{r}) \to 0$, as $\varepsilon_0 \to \infty$ yields

$$\frac{\Delta A^{\text{ch}}}{kT} = \int d\mathbf{r}_1 \sum_{\alpha=1}^{m} \rho_\alpha^{\text{seg}}(\mathbf{r}_1) \sum_{A}^{\{A\}} \left(-\frac{1}{2} \ln \int d\mathbf{r}_2 \times \exp[-\beta \nu_{\text{bond}}^{\alpha\alpha'}(\mathbf{r}_1, \mathbf{r}_2)] y^{\alpha\alpha'}(\mathbf{r}_1, \mathbf{r}_2) \rho_{\alpha'}^{\text{seg}}(\mathbf{r}_2) + \frac{1}{2} \right), \tag{4}$$

where the constant terms $\beta\varepsilon_0$ and $\ln K$ are dropped since they do not influence the phase behavior of the fully formed chains.

Since the reference fluid cavity correlation function for an inhomogeneous system is not known [8], we replace it by its bulk counterpart evaluated at a "coarse-grained density" $\overline{\rho}_\alpha^{\text{seg}}(\mathbf{r})$, i.e., $y^{\alpha\alpha'}(\mathbf{r}_1, \mathbf{r}_2, [\rho_1^{\text{seg}}, \ldots, \rho_m^{\text{seg}}]) = y^{\alpha\alpha',\text{bulk}}([\overline{\rho}_1^{\text{seg}}(\mathbf{r}_1), \ldots, \overline{\rho}_m^{\text{seg}}(\mathbf{r}_1)])$. The results we present here are from the simplest coarse-graining approximation, i.e., $\overline{\rho}_\alpha^{\text{seg}}(\mathbf{r}_1) = \frac{3}{4\pi\sigma_\alpha^3} \int_{|\mathbf{r}_1 - \mathbf{r}_2| < \sigma_\alpha} d\mathbf{r}_2 \rho_\alpha^{\text{seg}}(\mathbf{r}_2)$, for $\alpha = 1, \ldots, m$.

Figure 1 shows the average site density distribution of a freely jointed hard 20-mer ($\exp[-\beta \nu_{\text{bond}}^{\alpha\alpha'}(\mathbf{r}_1, \mathbf{r}_2)] = \frac{\delta(|\mathbf{r}_1 - \mathbf{r}_2| - \sigma^{\alpha\alpha'})}{4\pi(\sigma^{\alpha\alpha'})^2}$) near a hard surface, for two different packing fractions. The theory, in quantitative agreement with simulations, accurately captures the entropic (chain depletion) and energetic (chain enhancement) effects at low and high packing fractions, respectively. It is noteworthy that the calculations involve solving a set of first order integral equations regardless of the chain length. This is a significant simplification over the polymer DFTs based on molecular densities that entail solving coupled integral equations of order m (chain length) for calculations similar to those corresponding to Fig. 1. Consequently, these calculations become prohibitively expensive for higher chain lengths and for mixtures. The calculations from the present theory, on the other hand, are simple enough to be solved satisfactorily using elementary numerical techniques commonly used in atomic DFTs. Even with the simple Picard-type iteration, as described in [12], the computational cost and convergence characteristics were comparable to those of our earlier DF works on associating atomic fluids [12,14].

The theory can, in general, solve for the density distribution of each segment in the chain. However, this is usually not necessary, and it suffices to determine the end and middle segment distributions. Figure 2 shows these distributions for a flexible hard 20-mer. Similar predictions for athermal blends and solutions for a range of conditions are also found to be in agreement with simulations [20].

These athermal cases establish the capability of the theory to capture the packing effects due to chain connectivity and, hence, the accuracy of the chain functional. The impact of the molecular topological differences in a blend

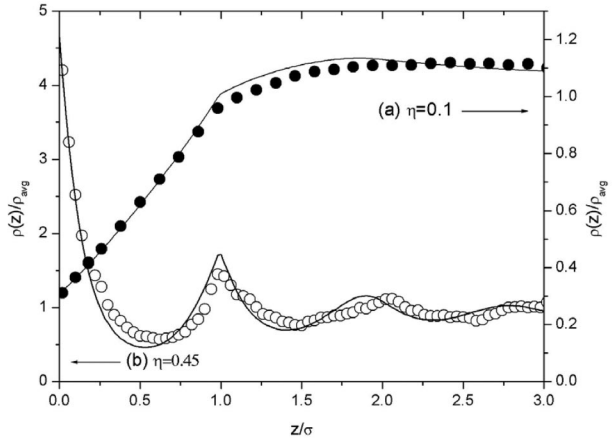

FIG. 1. Average segment-density profiles for a flexible hard 20-mer near a hard wall for packing fractions (a) 0.1 (filled circles, corresponding to the right axis), and (b) 0.45 (open circles, left axis). Lines are the theory predictions, and symbols are simulation data of Yethiraj *et al.* [27].

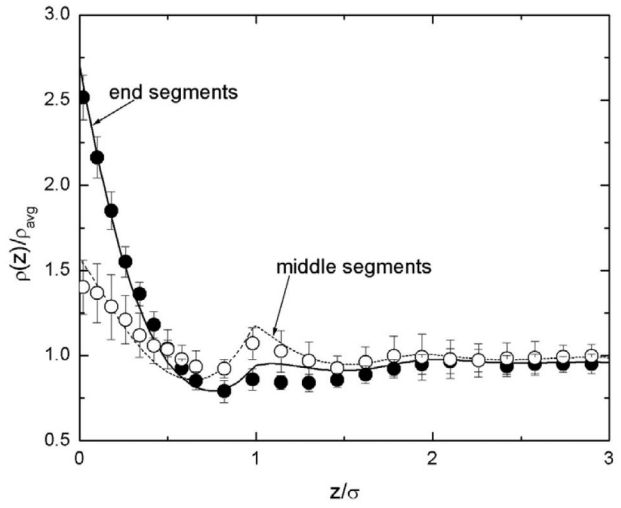

FIG. 2. End (filled circles and solid line) and middle (open circles and broken line) segment distribution in a flexible hard 20-mer chain near a hard wall for packing fraction 0.3. Lines are theory predictions and symbols are simulation data of Yethiraj *et al.* [27]. Error bars are shown for simulation results.

on the fluid structure has been studied through experiments [21,22] and simulations [23]; however, no theory has yet addressed it. In Fig. 3, we present the application of our theory for surface segregation in blends of linear and branched chains. In the athermal blend (inset), the entropic penalty keeps the branched chains away from the surface. In the presence of attraction between the polymer segments, the effective packing of the linear molecules against each other in the bulk leads to a stronger depletion of these chains at the surface. The theory captures this crossover from an entropy driven to an enthalpy driven segregation in agreement with the simulations. The theoretical calculations use the same model system (shown schematically in Fig. 3) and the site-site intermolecular potential as the simulations [23], $\beta u_{ff} = \infty\,(r<\sigma) = -\varepsilon_{ff}[\sigma e^{-\kappa(r/\sigma-1)}/r - e^{-\kappa}/2]\,(\sigma<r<2\sigma) = 0\,(r>2\sigma)$, where $\kappa = 2.5$ is the inverse range of shifted Yukawa potential. However, the intermolecular correlations accounted for in the simulations are ignored in the mean field approximation commonly used to treat attraction in the theory. This leads to different bulk conditions from the theory and the simulations, despite identical potential models. A comparison with simulations in the inhomogeneous region can be made only after the consistency of the bulk conditions between the theory and the simulations is ensured. We ascertain this by adjusting the attraction energy parameters for the two species, ε_{ff}, to match the corresponding partial pressures from the theory and the simulations. Once the *bulk* conditions are specified, the theory accurately maps out the structure of the branched and the linear species near the *surface*. It must be emphasized that the chain functional Eq. (4) remains unchanged in all of the above calculations.

The simplicity of the theory results from the exclusion of bonding constraints from the ideal system, obviating the use of multipoint density functions [1,6,7] or the intramolecular structure function [2] to describe it. These constraints enter through the chain functional Eq. (4), so that the free energy of an ideal heteronuclear tangent chain is given by

$$\frac{A^{\mathrm{id,ch}}}{kT} = \sum_{\alpha=1}^{m} \int d\mathbf{r}_1 \rho_\alpha^{\mathrm{seg}}(\mathbf{r}_1)\Big[\ln\rho_\alpha^{\mathrm{seg}}(\mathbf{r}_1) - 1 + \sum_{A}^{\{A\}}\Big(-\frac{1}{2} \times \ln\int d\mathbf{r}_2 \frac{\delta(|\mathbf{r}_1-\mathbf{r}_2|-\sigma^{\alpha\alpha'})}{4\pi(\sigma^{\alpha\alpha'})^2}\rho_{\alpha'}^{\mathrm{seg}}(\mathbf{r}_2) + \frac{1}{2}\Big)\Big]. \tag{5}$$

Notice that TPT1 automatically accounts for the connectivity between consecutive segments, a constraint that is normally forced through the ideal functionals in the existing theories [1,2,6,7]. This result is exact for a system of dimers, while the *formal* divergence from the exact free energy of an ideal chain [1] (obtained in terms of multipoint molecular density) at higher degrees of polymerization is due to the approximation introduced, which serves to decouple the mth-order integrals of the exact formalism. The resulting numerical difference, however, is insignificant even at relatively low densities ([as seen in the low density profiles in Fig. 1(a), compared to Fig. 4(a) of Ref. [6] which uses the exact ideal chain functional]. In fact, our theory is in better agreement with simulations than some of the theories using the exact ideal chain free energy (Figs. 3 and 5 of Ref. [8(c)]), due to better approximations for the excluded volume effects. At high packing

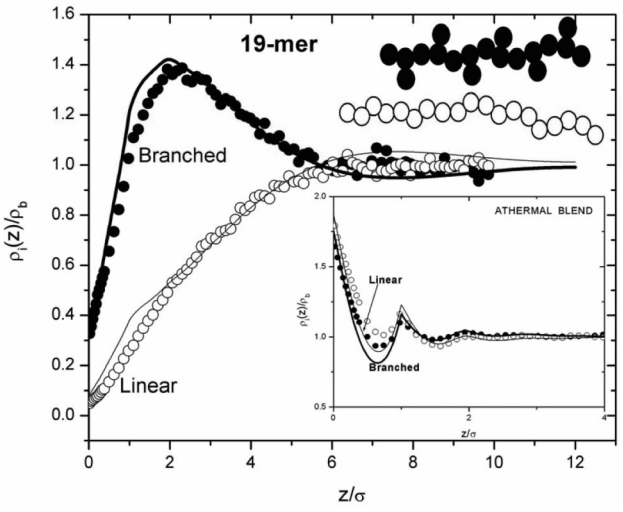

FIG. 3. Surface induced segregation of linear (open symbols and fine lines) and branched (filled symbols and bold lines) 19-mers in attractive and athermal (inset) blends near an athermal surface. Lines are theory predictions and symbols are simulation data of Yethiraj [23]. The topology of the two species is also shown schematically.

fractions, where the effect of single chain structure becomes insignificant (Flory's ideality principle [24]), the influence of this approximation fades away and the accuracy of the overall functional improves further. Polymer melts and high density polymer solutions thus do not justify the inconvenience of the exact formal treatment of the ideal chain functional.

In conclusion, we have derived a DFT to predict the structure and the thermodynamics of inhomogeneous polymeric solutions and blends. The theory provides accuracy comparable to the numerically intensive polymer DFTs, while retaining the simple form and the computational economy of DFTs for atomic fluids. Presented results project the theory as a thermodynamically consistent, versatile, and accurate framework to provide a molecular level understanding of a diverse set of systems such as surfactants, copolymers, colloids, etc. Also impressive is the feasibility of extensions to include additional interactions such as hydrogen bonding [12–14], polar, and electrostatic interactions within the same formalism. Their contributions to the free energy can be added as perturbations in Eq. (1) much the same way that has found success with SAFT among various homogeneous systems [25]. Recognizing that the structure of a homogeneous fluid can be obtained from the density distribution in the external field introduced by a single, arbitrarily chosen fluid particle in the system, as suggested by Percus [26], this theory can be used to determine the intermolecular and the intramolecular correlation functions of the bulk polyatomic systems.

The authors are indebted to Professor Arun Yethiraj for providing them with his simulation data, and also gratefully acknowledge the financial support of the Robert A. Welch Foundation.

[1] C. E. Woodward, J. Chem. Phys. **94**, 3183 (1991).
[2] (a) D. Chandler, J. D. McCoy, and S. J. Singer, J. Chem. Phys. **85**, 5971 (1986); (b) **85**, 5977 (1986); (c) J. D. McCoy, S. J. Singer, and D. Chandler, J. Chem. Phys. **87**, 4853 (1987).
[3] K. S. Schweizer and J. G. Curro, Phys. Rev. Lett. **58**, 246 (1987).
[4] K. S. Schweizer and J. G. Curro, Phys. Rev. Lett. **60**, 809 (1988).
[5] A. Yethiraj, J. Chem. Phys. **109**, 3269 (1998).
[6] Y. Yu and J. Wu, J. Chem. Phys. **117**, 2368 (2002).
[7] A. Yethiraj and C. E. Woodward, J. Chem. Phys. **102**, 5499 (1995).
[8] (a) E. Kierlik and M. L. Rosinberg, J. Chem. Phys. **97**, 9222 (1992); (b) **99**, 3950 (1993); (c) **100**, 1716 (1994).
[9] W. E. McMullen and K. F. Freed, J. Chem. Phys. **92**, 1413 (1990).
[10] C. E. Woodward, J. Chem. Phys. **97**, 4525 (1992); A. Yethiraj, Adv. Chem. Phys. **121**, 89 (2002).
[11] (a) M. S. Wertheim, J. Stat. Phys. **35**, 19 (1984); (b) **35**, 35 (1984); (c) **42**, 459 (1986); (d) **42**, 477 (1986).
[12] C. J. Segura and W. G. Chapman, Mol. Phys. **86**, 415 (1995); C. J. Segura, W. G. Chapman, and K. P. Shukla, Mol. Phys. **90**, 759 (1997).
[13] A. Patrykiejew, S. Sokolowski, and D. Henderson, Mol. Phys. **97**, 919 (1999).
[14] (a) S. Tripathi and W. G. Chapman, J. Chem. Phys. **118**, 7993 (2003); (b) **119**, 12 611 (2003).
[15] W. G. Chapman, G. Jackson, and K. E. Gubbins, Mol. Phys. **65**, 1057 (1988); G. Jackson, W. G. Chapman, and K. E. Gubbins, Mol. Phys. **65**, 1 (1988).
[16] R. Evans, *Fundamentals of Inhomogeneous Fluids* (Marcel-Dekker, New York, 1992).
[17] T. F. Meister and D. M. Kroll, Phys. Rev. A **31**, 4055 (1985).
[18] P. Tarazona, U. M. B. Marconi, and R. Evans, Mol. Phys. **60**, 573 (1987).
[19] Y. Rosenfeld, Phys. Rev. Lett. **63**, 980 (1989).
[20] S. Tripathi and W. G. Chapman, J. Chem. Phys. (to be published).
[21] U. Steiner *et al.*, Science **258**, 1126 (1992).
[22] M. Sikka *et al.*, Phys. Rev. Lett. **70**, 307 (1993).
[23] A. Yethiraj, Phys. Rev. Lett. **74**, 2018 (1995).
[24] P. J. Flory, *Statistical Mechanics of Chain Molecules* (Interscience Publishers, New York, 1969).
[25] E. A. Muller and K. E. Gubbins, Ind. Eng. Chem. Res. **40**, 2193 (2001).
[26] J. P. Hansen and I. R. McDonald, *Theory of Simple Fluids* (Academic Press, New York, 1986).
[27] A. Yethiraj and C. K. Hall, Macromolecules **23**, 1865 (1990).